

Exploiting shot noise correlations in the photodetection of ultrashort optical pulse trains

F. Quinlan^{1*}, T. M. Fortier¹, H. Jiang¹, A. Hati¹, C. Nelson¹, Y. Fu², J. C. Campbell² and S. A. Diddams^{1*}

Photocurrent shot noise represents the fundamental quantum limit for amplitude, phase and timing measurements of optical signals. It is generally assumed that non-classical states of light must be employed to alter the standard, time-invariant shot noise detection limit. However, in the detection of periodic signals, correlations in the shot noise spectrum can impact the quantum limit of detection. Here, we show how these correlations can be exploited to improve shot noise-limited optical pulse timing measurements by several orders of magnitude. This has allowed us to realize a photodetected pulse train timing noise floor at an unprecedented 25 zs Hz^{-1/2} (corresponding phase noise of -179 dBc Hz⁻¹ on a 10 GHz carrier), ~5 dB below the level predicted by the accepted time-invariant shot noise behaviour. This new understanding of the shot noise of time-varying signals can be used to greatly improve photonic systems, affecting a wide range of communication¹, navigation² and precision measurement³ applications.

Shot noise results from the discrete nature of the detection of optical fields. There is a fundamental randomness of photon flux that, upon photodetection, is transformed into fluctuations in the photocurrent known as shot noise⁴. Whether the light is continuous wave or has a periodically varying intensity, the shot noise spectral density is a well-defined quantity, allowing a useful frequency-domain description. In either case, the shot noise current spectral density (units A² Hz⁻¹) is $2qI_{\text{avg}}$, where q is the fundamental charge and I_{avg} is the average photocurrent⁵. In the absence of quantum-mechanically squeezed states of light⁶, this expression is considered to dictate the fundamental limit to the achievable signal-to-noise in photocurrent measurements.

Even for classical light fields, however, $2qI_{\text{avg}}$ is not a complete description of the shot noise, as it does not provide information on possible phase correlations in the noise spectrum. The impact of spectral correlations is often overlooked, because, for continuous wave signals, no correlations are present. On the other hand, signals with periodically varying intensity do produce spectral correlations in the shot noise, with consequences for the shot noise limit of measurements of the optical field. For example, such correlations have been shown to degrade the noise floor in some gravitational wave detectors by ~2 dB (ref. 7). Until now, it has gone unrecognized that these correlations can result in orders of magnitude improvement in the quantum limit of the timing precision of a train of photodetected ultrashort pulses. Our measurements confirm our prediction that shot noise can be manipulated such that the pulse-to-pulse timing precision can be significantly improved simply by keeping the optical pulse width at the detector sufficiently short.

Previous studies on the shot noise of time-varying signals have not addressed the detection of ultrashort pulses⁷⁻¹². This is due in part to the fact that, until recently, the power-handling capability

of high-speed photodetectors has been insufficient to operate well within the shot noise limit at microwave frequencies. Photodetection of a train of ultrashort pulses (for example, the output of a mode-locked laser) produces microwave tones at harmonics of the pulse repetition rate f_r . The pulse train timing jitter is determined by measuring the phase noise sidebands of these harmonics¹³. Without sufficient microwave power, the signal-to-noise ratio is limited by thermal noise, and no optical pulse width dependence on phase noise is detectable.

To understand the optical pulse width dependence of the photocurrent shot noise-limited timing precision, it is useful to start with the pulse-to-pulse timing jitter at the fundamental limit imposed by the discrete nature of photons. From pulse to pulse, there are random variations in both the number of photons per pulse and the photon distribution within a pulse. Randomness in the photon distribution produces small deviations in the time of arrival of the pulse, or timing jitter, which may be thought of as variations in the arrival of the pulse 'centre of mass'. The shorter the optical pulse, the smaller the jitter, because there is a smaller pull on the pulse centre when the photons are more tightly packed¹⁴ (Supplementary Section S1). This is illustrated in the pulse ensemble of Fig. 1a by noting the difference in the thickness of the rising edge of the short and broad pulse ensembles.

Photodetection produces a train of much broader current pulses with a minimum timing jitter due to shot noise. Conceptually, the pulse-to-pulse timing instability is revealed by comparing (multiplying) the photodetected signal with the zero-crossing of a timing reference¹⁵, as shown in Fig. 1b. The shot noise is not constant, but arrives in bursts along with the pulses. Multiplying the zero-crossings with the shot noise bursts results in lower noise power, and therefore improved timing precision, for shorter pulses.

Although Fig. 1b suggests a pulse width dependence, it is not immediately clear whether the impact of photocurrent shot noise on timing measurements scales with the optical pulse width or the much broader electrical pulse. Because the phase noise of the photonically generated microwave harmonics represents the optical pulse timing jitter, it is the optical pulse width that must determine the fundamental timing precision in a photocurrent measurement. A time-varying photocurrent analysis at the shot noise limit shows that this is indeed the case, predicting an imbalance of the shot noise between amplitude and phase quadratures of the phototonically generated microwave harmonics (Supplementary Section S2).

The unequal distribution between the amplitude and phase quadratures is key to understanding how shot noise limits the timing precision, so we have developed an intuitive interpretation of how this imbalance arises. Shot noise may be viewed as the result of heterodyne beat signals between the optical signal and vacuum fluctuations^{16,17} (Fig. 2). In the frequency domain, an optical pulse train is represented as a frequency comb with a fixed

¹National Institute of Standards and Technology, 325 Broadway, Boulder, Colorado 80305, USA, ²Department of Electrical Engineering, University of Virginia, Charlottesville, Virginia 22904, USA. *e-mail: franklyn.quinlan@nist.gov; scott.diddams@nist.gov

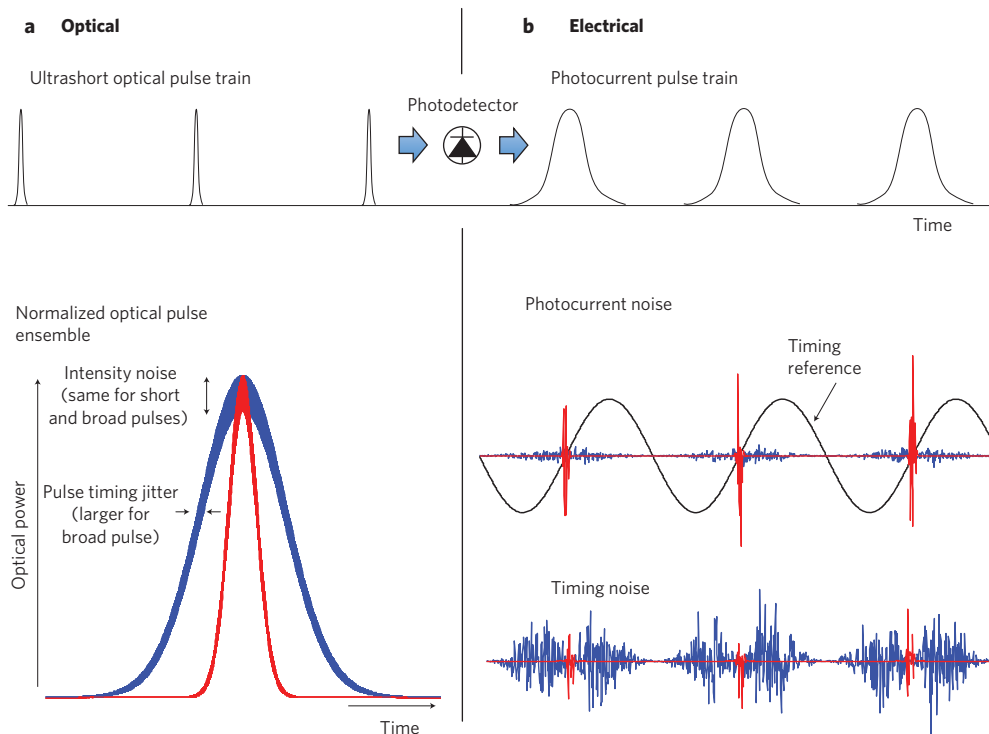


Figure 1 | Fluctuations and shot noise in the time domain. **a**, An ultrashort optical pulse train exhibits pulse-to-pulse amplitude and timing noise due to quantum fluctuations. A normalized ensemble of pulses shows the timing jitter dependence on optical pulse width. **b**, Photodetection produces a train of electrical pulses with shot noise. The time-averaged current variance is given by the average photocurrent, leading to larger peak variations in the shot noise for shorter pulses (in red) for the same average power. Multiplying the shot noise current by a phase reference reveals how shorter optical pulses yield a lower timing noise power.

phase among the comb lines. Vacuum fluctuations are represented as an uncorrelated continuous background. Photodetection generates heterodyne beat signals among the comb lines at multiples of f_r , as well as between the vacuum fluctuations and the comb. At any particular photocurrent frequency, the shot noise is the result of comb lines beating with all vacuum modes that are offset from a comb line by the same frequency. Also, each vacuum mode is translated to various photocurrent frequencies due to its beating with multiple comb lines. This results in correlations in the shot noise photocurrent at different frequencies, because the comb lines are phase-correlated. The degree of correlation between two photocurrent frequencies is determined by the fraction of the shot noise that is due to the same vacuum modes that appear at both frequencies. The shot noise will never be fully correlated, because, at any photocurrent frequency, there are always vacuum modes outside the comb bandwidth that only beat with a single comb line. Moreover, the degree of correlation is a function of the relative phase among comb lines, such that a chirped pulse has a reduced degree of correlation relative to an unchirped pulse. The dependence is therefore most simply described in terms of the temporal width of the optical pulse intensity profile.

Important for timing measurements is the fact that the shot noise sidebands symmetric about harmonics of f_r are correlated (Fig. 2). Positive correlations of the microwave carrier's upper and lower sidebands produce an imbalance between the amplitude and phase noise, shifting the shot noise out of the phase quadrature and into the amplitude quadrature. As a simple example, consider an optical spectrum consisting of N lines of equal intensity and in phase. Because only the vacuum noise mixing with the highest and lowest frequency comb lines contributes uncorrelated noise, the correlation between upper and lower sidebands about f_r is $(N - 2)/N$. This represents the fraction of the shot noise

that is shifted to the amplitude noise, reducing the phase noise to $1 - (N - 2)/N$.

We have derived the impact of these correlations for an arbitrary pulse train (Supplementary Section S2). The resulting shot noise-limited single-sideband phase noise-to-microwave power ratio at frequency f_r is

$$L_\phi = \frac{qI_{\text{avg}}R|H_n(f_r)|^2}{P(f_r)} [1 - C(\tau)] \quad [\text{Hz}^{-1}] \quad (1)$$

where $P(f_r)$ is the power of the photonic generated microwave signal, $H_n(f_r)$ is the value of the photodetector transfer function at f_r , R is the system impedance, τ is the optical pulse width, and $C(\tau)$ is the optical pulse width-dependent degree of correlation between upper and lower sidebands, ranging from 0 ($\tau \rightarrow 1/f_r$) to 1 ($\tau \rightarrow 0$). The correlation function depends on the particular pulse shape and, for Gaussian-shaped optical pulses, is given by $\exp\{- (2\pi f_r \tau)^2\}$.

The term in brackets in equation (1) may be considered as the pulse-width-dependent improvement in the shot noise-limited phase noise floor. Figure 3a plots the calculated sensitivity improvement on a 10 GHz microwave carrier for Gaussian-shaped pulses as a function of pulse width. For an optical pulse width of 1 ps, the phase noise quadrature of the shot noise is suppressed by ~ 30 dB. If, for example, we also had an average photocurrent of 15 mA and a 10 GHz carrier power of +10 dBm (typical levels for our photodetectors¹⁸), the shot noise limit would be -200 dBc Hz^{-1} . For lower frequency harmonics of f_r , the shot noise contribution to the phase noise is predicted to be even lower. For the same +10 dBm microwave carrier power, the room-temperature thermal limit on the phase noise would be -187 dBc Hz^{-1}

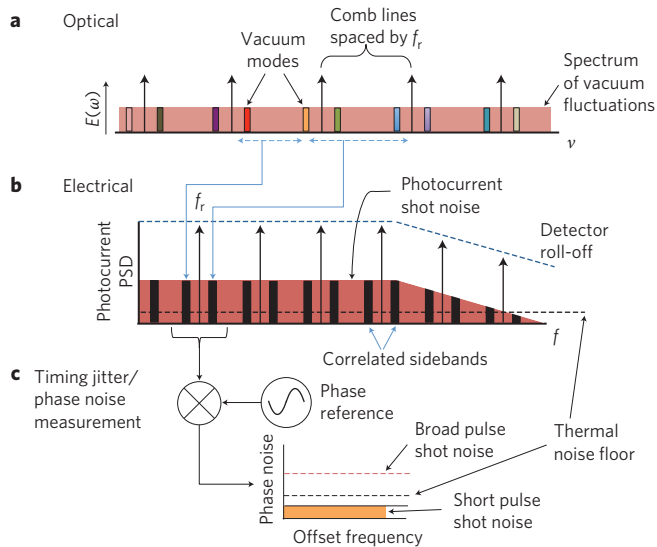


Figure 2 | Shot noise in the frequency domain. **a**, An optical frequency comb and vacuum fluctuations that heterodyne, or ‘beat’, to produce shot noise in the photocurrent. **b**, Correlations in the photocurrent spectrum arise due to the beating of vacuum fluctuations with multiple comb lines. **c**, In timing jitter/phase noise measurements, a harmonic of f_r is selected and compared to a phase reference. Sidebands about f_r harmonics are correlated, producing an imbalance between amplitude and phase noise. For ultrashort optical pulses, shot noise in the phase quadrature is orders of magnitude below the total photocurrent shot noise PSD.

(ref. 19). Thus, for short optical pulses, the shot noise impact on the timing precision can be made negligible. This improvement in the shot noise-limited timing precision comes at the slight cost of a ≤ 3 dB increase in the amplitude noise of the photonically generated microwave signal.

Measurements were performed to confirm our analysis. A 2 GHz repetition rate pulse train from a Ti:sapphire mode-locked laser illuminated a high-speed photodiode designed for high power handling and high linearity¹⁸, with an impulse response time of ~ 34 ps. Before measuring the phase noise, the photocurrent power spectral density (PSD) was measured, confirming that the directly detected photocurrent was shot-noise limited (see Methods), as depicted in Fig. 2b. Phase noise measurements were performed on the fifth harmonic of the repetition rate at 10 GHz. For offset frequencies of 1–10 MHz, the technical noise from the mode-locked laser is below the measurement noise floor. Our phase noise measurements therefore concentrated on this frequency range. The phase noise was measured for different optical pulse lengths at the detector, obtained by dispersive broadening in the optical fibre (this varied the relative phase among the comb lines). Phase noise measurements are shown in Fig. 3b. Measurements for 1 ps optical pulses reached a noise floor at -179 dBc Hz⁻¹, or ~ 5 dB below the long pulse shot noise limit, and 10–20 dB below previous photonic approaches to low-phase-noise microwaves^{20–23}. In terms of pulse timing precision, this noise floor corresponds to only 25 zs Hz^{-1/2}, which is 3 dB above the measurement system limit of -182 dBc Hz⁻¹. The source of this difference is currently under investigation, and possibilities include increased thermal noise due to heating of the photodetection active area, which our modelling shows can reach temperatures greater than 500 K, and noise on the photodetector’s bias voltage.

The measured sensitivity improvement over the long pulse limit for all measurements is shown in Fig. 3a together with our calculation. Adding the measured noise floor to the calculation puts our measurements in close agreement with the prediction, shown as the dashed curve in Fig. 3a.

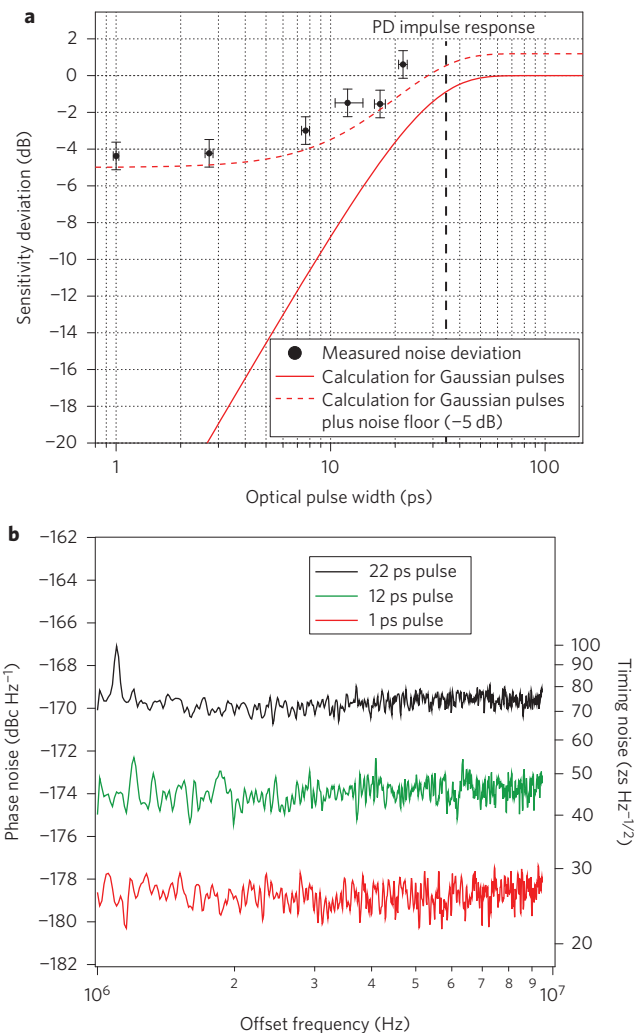


Figure 3 | Phase noise prediction and measurement of a photonically generated 10 GHz signal. **a**, Phase sensitivity deviation from the long pulse limit calculated for a Gaussian-shaped optical pulse (solid curve) and the calculation with the added noise floor of -179 dBc Hz⁻¹ (dashed curve). Measurements are plotted as black points. Vertical error bars result from uncertainty in the detector roll-off and variance in the phase noise measurement. Horizontal error bars result from uncertainty in the pulse width. The vertical dashed line indicates the photodetector (PD) impulse response. **b**, Measured phase noise for selected optical pulse widths.

High-speed photodetectors can now achieve microwave powers approaching 1 W (ref. 24). In this case, equation (1) predicts that the phase noise limit at 10 GHz due to shot noise for a 1 ps pulse train is ~ -209 dBc Hz⁻¹. The thermal noise floor is only slightly above this. At this level, the microwave phase stability derived from photonic techniques would far surpass the best electronic sources on even the shortest of timescales. Reaching a signal-to-noise ratio of nearly 21 orders of magnitude will certainly require understanding and overcoming a variety of other technical challenges. However, with a path to mitigate shot noise now clear, we enter a new regime that will undoubtedly provide insights into ultra-low-noise metrology and photodetection physics, and should lead to an even wider use of photonics in applications traditionally performed by electronic oscillators.

Methods

Optical pulse source. A 1 GHz repetition rate, octave-spanning Ti:sapphire mode-locked laser was used as the pulse source²⁵. Before photodetection, this repetition

rate was doubled by pulse interleaving^{22,26}. This moved the onset of saturation to a photocurrent level well above our operating conditions (discussed in the 'Photodetection' section). An acousto-optic modulator (AOM) was placed in the beam path to aid with measurements of amplitude-to-phase conversion in the photodetector^{27,28}. Minimization of amplitude-to-phase conversion was critical to achieve the low phase noise floors. The pulse duration after the AOM was ~ 1 ps. The optical spectrum sent to the photodetector was centred at 980 nm, with a width of ~ 50 nm. The fibre used to vary the optical pulse duration was single mode at 980 nm, and fibres with lengths of 1 m, 3 m, 6 m, 11 m and 16 m were used to dispersively broaden the optical pulses. The optical pulse widths for the various fibre lengths were determined by a combination of intensity autocorrelation and high-speed photodetectors. Uncertainties in the pulse width arise from incomplete knowledge of the pulse shape. The optical pulse width uncertainties are reflected in the horizontal error bars in Fig. 3a.

Photodetection. The photodetectors used in this work were of a modified uni-travelling carrier design, built for high linearity and high power handling¹⁸. The average photocurrent ranged between 14 mA and 18 mA for all phase noise measurements. The bias voltage ranged between 15 V and 21 V. For each measurement, the voltage used was that which minimized amplitude-to-phase conversion in the photodetector. The photodetected power at 10 GHz was ~ 10 dBm in a 50 Ω system. No saturation of the 10 GHz power was detectable for photocurrents less than 25 mA. An important factor for correct calculation of the shot noise deviation was the transfer function of the photodiode. Two methods were used to calculate this as accurately as possible. First, the power in the 2 GHz and 10 GHz tones were compared to the d.c. power under short pulse illumination. When the incident optical pulse is much shorter than the impulse response of the detector, the roll-off in power of the repetition rate harmonics is only due to the transfer function of the detector. Second, the photocurrent noise as a function of average photocurrent was measured near d.c., near 2 GHz and near 10 GHz for all fibre lengths. No dependence on optical pulse width was observed. The near d.c. photocurrent noise measurements were consistent with $2qI_{\text{avg}}R$. In the shot noise limit, the only difference among the noise power levels at different centre frequencies is due to the roll-off in the photodetector response. Both shot noise and microwave tone power measurements were consistent within 0.5 dB. The uncertainty in the photodetector transfer function is reflected in the vertical error bars of Fig. 3a. More details regarding photodetector requirements for realizing orders-of-magnitude improvement in the shot noise-limited phase noise are given in Supplementary Section S3.

Phase noise measurement. Phase noise measurements are presented in units of dBc Hz⁻¹, that is, the base 10 logarithm of the single-sideband phase noise power, relative to the power of the 10 GHz harmonic, in a 1 Hz bandwidth. Phase noise measurements were performed by comparing the photodetected 10 GHz signal with an ultrastable phase reference²⁹ (phase noise is ~ 190 dBc Hz⁻¹ from 1 MHz to 10 MHz) using a phase bridge¹⁵. A cross-correlation measurement technique³⁰ was required to achieve a measurement noise floor of -182 dBc Hz⁻¹, limited by the available 10 GHz power from the photodiode. This was verified by applying a separate 10 GHz ultrastable phase reference with microwave power the same as the photonically generated signal. The phase noise measurement was calibrated with the single-sideband calibration technique. A phase lock with a bandwidth less than 10 kHz was used between the phase reference and the photodetected signal to maintain phase quadrature during the measurement. As our phase noise measurements focused on offset frequencies greater than 1 MHz, there was no influence of the phase lock on the results. Finite variance of the noise spectrum resulted in some uncertainty in the phase noise level. This uncertainty is also reflected in the vertical error bars of Fig. 3a. Amplitude noise on the 10 GHz harmonic of ~ -170 dBc Hz⁻¹ in the 1–10 MHz offset range was also measured.

Received 10 September 2012; accepted 30 January 2013;
published online 10 March 2013

References

1. Armada, A. G. Understanding the effects of phase noise in orthogonal frequency division multiplexing (OFDM). *IEEE Trans. Broadcast.* **47**, 153–159 (2001).
2. Scheer, J. A. & Kurtz, J. L. *Coherent Radar Performance Estimation* (Artech House, 1993).
3. Santarelli, G. *et al.* Frequency stability degradation of an oscillator slaved to a periodically interrogated atomic resonator. *IEEE Trans. Ultrason. Ferroelectr. Freq. Control* **45**, 887–894 (1998).
4. Yariv, A. in *Optical Electronics in Modern Communications* 5th edn, Ch. 10 (Oxford Univ. Press, 1997).
5. Boyd, R. W. in *Radiometry and the Detection of Optical Radiation* Ch. 4 (Wiley, 1983).
6. Walls, D. F. Squeezed states of light. *Nature* **306**, 141–146 (1983).

7. Niebauer, T. M., Schilling, R., Danzmann, K., Rudiger, A. & Winkler, W. Nonstationary shot noise and its effect on the sensitivity of interferometers. *Phys. Rev. A* **43**, 5022–5029 (1991).
8. Bruyevich, A. N. Fluctuations in autooscillators for periodically nonstationary shot noise. *Telecomm. Radio Eng.* **23**, 91–96 (1968).
9. Gray, M. B., Stevenson, A. J., Bachor, H. A. & McClelland, D. E. Harmonic demodulation of nonstationary shot noise. *Opt. Lett.* **18**, 759–761 (1993).
10. Meers, B. J. & Strain, K. A. Modulation, signal, and quantum noise in interferometers. *Phys. Rev. A* **44**, 4693–4703 (1991).
11. Winzer, P. J. Shot-noise formula for time-varying photon rates: a general derivation. *J. Opt. Soc. Am. B* **14**, 2424–2429 (1997).
12. Rakhmanov, M. Demodulation of intensity and shot noise in the optical heterodyne detection of laser interferometers for gravitational waves. *Appl. Opt.* **40**, 6596–6605 (2001).
13. von der Linde, D. Characterization of the noise in continuously operating mode-locked lasers. *Appl. Phys. B* **39**, 201–217 (1986).
14. Paschotta, R. Noise of mode-locked lasers (Part II): timing jitter and other fluctuations. *Appl. Phys. B* **79**, 163–173 (2004).
15. *Characterization of Clocks and Oscillators: NIST Technical Note 1337* (US GPO, 1990).
16. Bachor, H. A. & Manson, P. J. Practical implications of quantum noise. *J. Mod. Opt.* **37**, 1727–1740 (1990).
17. Henry, C. H. & Kazarinov, R. F. Quantum noise in photonics. *Rev. Mod. Phys.* **68**, 801–853 (1996).
18. Li, Z., Pan, H. P., Chen, H., Beling, A. & Campbell, J. C. High-saturation-current modified uni-traveling-carrier photodiode with cliff layer. *IEEE J. Quantum Electron.* **46**, 626–632 (2010).
19. Hati, A., Howe, D. A., Walls, F. L. & Walker, D. K. Merits of PM noise measurement over noise figure: a study at microwave frequencies. *IEEE Trans. Ultrason. Ferroelectr. Freq. Contr.* **53**, 1889–1894 (2006).
20. Eliyahu, D., Seidel, D. & Maleki, L. in *Proceedings of the IEEE International Frequency Control Symposium* 811–814 (IEEE, 2008).
21. Fortier, T. M. *et al.* Generation of ultrastable microwaves via optical frequency division. *Nature Photon.* **5**, 425–429 (2011).
22. Haboucha, A. *et al.* Optical-fiber pulse rate multiplier for ultralow phase-noise signal generation. *Opt. Lett.* **36**, 3654–3656 (2011).
23. Jiang, H. *et al.* in *Proceedings of the IEEE International Frequency Control Symposium* (IEEE, 2012).
24. Li, Z. *et al.* High-power high-linearity flip-chip bonded modified uni-traveling carrier photodiode. *Opt. Express* **19**, 385–390 (2011).
25. Fortier, T. M., Bartels, A. & Diddams, S. A. Octave-spanning Ti:sapphire laser with a repetition rate >1 GHz for optical frequency measurements and comparisons. *Opt. Lett.* **31**, 1011–1013 (2006).
26. Jiang, H. F., Taylor, J., Quinlan, F., Fortier, T. & Diddams, S. A. Noise floor reduction of an Er:fiber laser-based photonic microwave generator. *IEEE Photon. J.* **3**, 1004–1012 (2011).
27. Taylor, J. *et al.* Characterization of power-to-phase conversion in high-speed P-I-N photodiodes. *IEEE Photon. J.* **3**, 140–151 (2011).
28. Zhang, W. *et al.* Amplitude to phase conversion of InGaAs pin photo-diodes for femtosecond lasers microwave signal generation. *Appl. Phys. B* **106**, 301–308 (2012).
29. Fortier, T. M. *et al.* Sub-femtosecond absolute timing jitter with a 10 GHz hybrid photonic-microwave oscillator. *Appl. Phys. Lett.* **100**, 231111 (2012).
30. Walls, W. F. in *Proceedings of the IEEE Frequency Control Symposium* 257–261 (IEEE, 1992).

Acknowledgements

The authors thank P. Winzer, S. Papp, N. Newbury, E. Ivanov, R. Mhaskar, A. Ludlow and J. Bergquist for useful discussions and comments on this manuscript. This work was supported by the National Institute of Standards and Technology and in part by the Defense Advanced Research Projects Agency. It is a contribution of an agency of the US Government and is not subject to copyright in the USA.

Author contributions

F.Q., T.M.F., H.J. and S.A.D. developed the model. F.Q., T.M.F., A.H., C.N. and S.A.D. performed the measurements. Y.F. and J.C. designed, modelled and fabricated the photodetectors. F.Q., T.M.F. and S.A.D. analysed the data and prepared the manuscript.

Additional information

Supplementary information is available in the online version of the paper. Reprints and permissions information is available online at www.nature.com/reprints. Correspondence and requests for materials should be addressed to F.Q. and S.A.D.

Competing financial interests

The authors declare no competing financial interests.